

# Characteristics of the Boundary Model in Two-Dimensional NS-FDTD Method

Tadao Ohtani<sup>1</sup> and Yasushi Kanai<sup>2</sup>

<sup>1</sup>1-9-5 Kakeage, Minami-ku, Nagoya 457-0007, Japan

<sup>2</sup>Niigata Institute of Technology, Kashiwazaki 945-1195, Japan

E-mail: kanai@iee.niit.ac.jp

**Abstract** — This paper investigates the representation of the dielectric boundary and absorbing boundary conditions (ABC) in the nonstandard FDTD (NS-FDTD) method. The effective permittivity model of the boundary is examined and it is found that its accuracy decreases when the dielectric boundary coincides with a node. To overcome this difficulty, we propose an alternative, highly accurate boundary model. The accuracy of the perfectly matched layer (PML) as an ABC is also demonstrated in the NS-FDTD algorithm.

## I. INTRODUCTION

The NS-FDTD method is a time-domain analysis technique for electromagnetic waves with a fixed frequency [1]. The solution error is less than  $10^{-4}$  that of the standard FDTD method on a coarse grid. However, the accuracy of the method is only preserved in homogeneous media. When dielectric interfaces exist in the calculation area the accuracy of the NS-FDTD method is dependent on the accuracy of the media boundary model. A rigorous boundary model based on the NS-FDTD algorithm has not been developed yet, therefore, the effective permittivity model [2] originally developed for the FDTD method has been applied to the NS-FDTD analysis [1]. Same discussion stands for PML [3]. However, the validity of this approach for NS-FDTD calculations has not been verified.

In this paper, we examine the validity of the effective permittivity boundary model by using a two-dimensional NS-FDTD analysis of a dielectric slab. It is found that the model has poor accuracy when the interface coincides with a node. To overcome the difficulty, we propose an accurate boundary model based on the continuity of the fields along the boundary. It is shown that our method can reduce the error of the effective permittivity boundary model. For analysis of open regions the characteristics of the PML [3] are also investigated.

## II. CHARACTERISTIC OF THE DIELECTRIC BOUNDARY MODEL

### A. Effective Permittivity Model

Fig. 1 shows the effective permittivity model [2] using the fractions of  $\epsilon_{1,2}$  in the cell for the FDTD method. Fig. 2 indicates the relative positions of the boundary and  $E, H$ -field nodes. In Fig. 3, the transmission rate versus incident angle is shown for  $\delta = \Delta/4$  and  $\delta = 0$  obtained by various methods along with the reference value obtained by the transmission matrix method [4]. It is seen that the effective permittivity model agrees well with reference value when  $\delta = \Delta/4$ , however, the accuracy is low when  $\delta = 0$ .

### B. Proposed Boundary Model

In order to overcome the low accuracy when  $\delta = 0$ , we propose a model based on the continuity of the tangential and

time derivative components of the fields on the boundary [5]. We introduce the virtual fields,  $\tilde{H}_y^{(i)}(x+\Delta/2)$  and  $\tilde{E}_z^{(i)}(x+\Delta/2)$ , straddling the interface for the NS-FDTD calculation of  $\epsilon_r^{(i)}$ -side. They are given as

$$\tilde{\epsilon}_r = V_1 \epsilon_1 + V_2 \epsilon_2 \quad 1/\tilde{\epsilon}_r = V_1/\epsilon_1 + V_2/\epsilon_2$$

Fig. 1. The effective permittivity  $\tilde{\epsilon}_r$  model for the FDTD method [2]. Here,  $V_{1,2}$  are the fractions of  $\epsilon_{1,2}$  in cell.

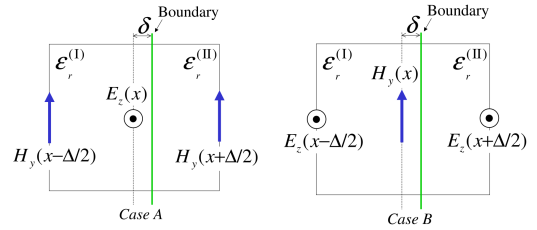


Fig. 2. Relative positions of the dielectric boundary and  $E, H$ -field nodes for  $TM_z$  mode in cell.  $\delta$  is the offset from center node of cell to dielectric boundary.

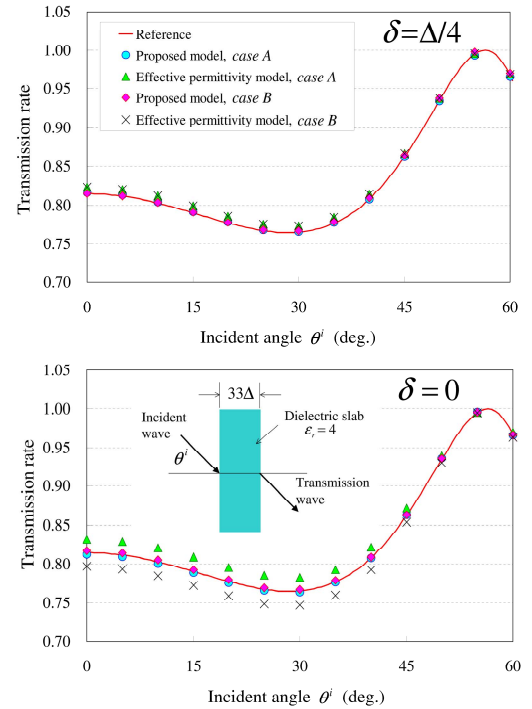


Fig. 3. Comparison with the effective permittivity model and our proposed model with  $N=3$  and  $M=2$  in the analysis of a dielectric slab by the NS-FDTD method with  $\Delta = \lambda/20$ . Here, the effective permittivity model is the parallel case (a) in Fig. 1.

$$\tilde{H}_y^{(1)}(x+\Delta/2) = \left[ a_{r0} \varepsilon_r^{(1)} \left\{ \sum_{n=1}^M b_{rn} H_y(x+\frac{2n-1}{2}\Delta) - \frac{\partial H_x}{\partial y} \right\} - a_{r0} \cdot \left\{ \sum_{n=1}^M b_{ln} H_y(x-\frac{2n-1}{2}\Delta) - \frac{\partial H_x}{\partial y} \right\} - b_{r0} \varepsilon_r^{(1)} \sum_{n=1}^M \left\{ a_{rn} H_y(x+\frac{2n-1}{2}\Delta) - a_{ln} f(x-\frac{2n-1}{2}\Delta) \right\} \right] / (\varepsilon_r^{(1)} a_{r0} b_{l0} - \varepsilon_r^{(1)} b_{r0} a_{l0}), \quad (1a)$$

$$\tilde{E}_z^{(1)}(x+\Delta/2) = \left[ b_{r0} \sum_{n=1}^N \left\{ a_{rn} E_z(x+\frac{2n-1}{2}\Delta) - a_{ln} E_z(x-\frac{2n-1}{2}\Delta) \right\} - a_{r0} \cdot \sum_{n=1}^M \left\{ b_{rn} E_z(x+\frac{2n-1}{2}\Delta) - b_{ln} E_z(x-\frac{2n-1}{2}\Delta) \right\} \right] / (a_{l0} b_{r0} - b_{l0} a_{r0}), \quad (1b)$$

where (1a) is for *case A* and (1b) is for *case B* in Fig. 2.  $\tilde{H}_y^{(1)}(x-\Delta/2)$  and  $\tilde{E}_z^{(1)}(x-\Delta/2)$  for  $\varepsilon_r^{(1)}$ -side can be derived in the same manner. The derivations of  $a_{rn}$ ,  $b_{rn}$ , and (1) are shown in the appendix. Here,  $N=3$  and  $M=2$  were used in (1). It is seen in Fig. 3 that our model can reduce the error of the effective permittivity model when the dielectric interface is on an *E* or *H*-node.

### III. CHARACTERISTICS OF THE PML

Fig. 4 shows the reflection rate of the field-splitting type PML in the NS-FDTD method. The evaluation conditions of the PML are loss  $\sigma(x)=(x/d)^m \sigma$ ,  $\sigma_{opt} = -(m+1) \ln R(0)/2\eta d$  with  $R(0)=e^{-16}$  and  $\eta=\sqrt{\mu/\varepsilon}$  [3]. Although the variation of  $\sigma(x)$  that straddles two cells is ignored, the field-splitting type PML conditions for the FDTD method are valid in the NS-FDTD method. Values of  $m=3-4$  and  $\sigma \cong 0.75\sigma_{opt}$  are optimal as shown in Fig. 4.

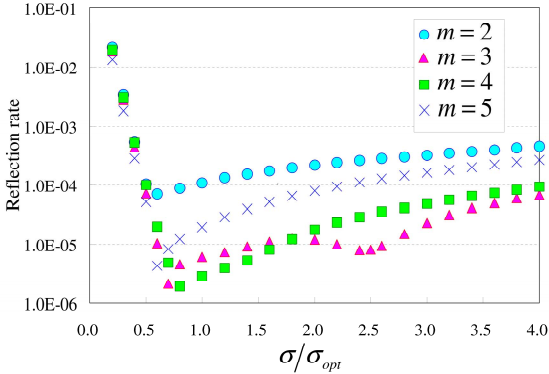


Fig. 4. Reflection rate of the field-splitting type PML in two-dimensional NS-FDTD method. PML width is  $d=10\Delta$ . Here,  $\Delta = \lambda/10$  and  $0^\circ$  incidence.

### IV. CONCLUSION

We have investigated the effective permittivity model (EPM) and PML boundary condition that are major concerns in the NS-FDTD method. It has been shown that EPM is useful in the NS-FDTD method, but the accuracy deteriorates when the boundary is on a node. To overcome this difficulty, we have proposed a useful complementary model for EPM. We have also studied the PML, and it has been confirmed numerically that the field-splitting type PML is valid in the NS-FDTD method.

### V. REFERENCES

- [1] J. B. Cole, "High accuracy nonstandard finite-difference time-domain algorithms for computational electromagnetics: Applications to optics and photonics," in *Advances in the Applications of Nonstandard Finite Difference Schemes*, R. E. Mickens, Ed. Singapore: World Scientific, 2005, Chapter 4, and its section 7.
- [2] T. Jalali et. al, "Efficient effective permittivity treatment for the 2D-FDTD simulation of photonic crystals," *Journal of Computational and Theoretical Nanoscience*, vol. 4, no. 3, pp. 644-648, 2007.
- [3] A. Taflove and S. C. Hangness, *Computational Electrodynamics: The Finite-Difference Time-Domain Method*, Norwood, MA: Artech House, 2000, Chapter 7.
- [4] C. A. Balanis, *Advanced Engineering Electromagnetics*, John Wiley & Sons, Inc., 1989, Chapter 5.
- [5] N. V. Kantartzis and T. D. Tsiboukis, *Higher-order FDTD schemes for waveguide and antenna structures*, San Rafael, CA, USA: Morgan & Claypool Publishers, 2006, Chapter 2.

### APPENDIX

In Fig. 2, the value of  $f(x+\delta)$  on the boundary is expressed by using a Taylor series. For third order ( $N=3$ ) approximation,

$$\begin{aligned} f(x-\frac{\Delta}{2}) &= f(x+\delta) - \left(\frac{\Delta}{2} + \delta\right) f^{(1)} + \frac{1}{2!} \left(\frac{\Delta}{2} + \delta\right)^2 f^{(2)} - \frac{1}{3!} \left(\frac{\Delta}{2} + \delta\right)^3 f^{(3)}, \\ f(x+\frac{\Delta}{2}) &= f(x+\delta) + \left(\frac{\Delta}{2} - \delta\right) f^{(1)} + \frac{1}{2!} \left(\frac{\Delta}{2} - \delta\right)^2 f^{(2)} + \frac{1}{3!} \left(\frac{\Delta}{2} - \delta\right)^3 f^{(3)}, \\ f(x+\frac{3\Delta}{2}) &= f(x+\delta) + \left(\frac{3\Delta}{2} - \delta\right) f^{(1)} + \frac{1}{2!} \left(\frac{3\Delta}{2} - \delta\right)^2 f^{(2)} + \frac{1}{3!} \left(\frac{3\Delta}{2} - \delta\right)^3 f^{(3)}, \\ f(x+\frac{5\Delta}{2}) &= f(x+\delta) + \left(\frac{5\Delta}{2} - \delta\right) f^{(1)} + \frac{1}{2!} \left(\frac{5\Delta}{2} - \delta\right)^2 f^{(2)} + \frac{1}{3!} \left(\frac{5\Delta}{2} - \delta\right)^3 f^{(3)}. \end{aligned} \quad (2)$$

$f^R(x+\delta)$  is obtained from (2) of right-hand side nodes in Fig. 2. Here,  $f^{(n)} = \partial^n f(x)/\partial x^n|_{x=x+\delta}$ . In a similar manner,  $f^L(x+\delta)$  is given from  $f(x+\Delta/2)$  and  $f(x-(2n-1)\Delta/2)$  of left-hand side. By the continuity of  $f^R(x)=f^L(x)$ , we obtain generally

$$a_{l0} \tilde{f}^{(1)}(x+\frac{\Delta}{2}) - a_{r0} \tilde{f}^{(1)}(x-\frac{\Delta}{2}) = \sum_{n=1}^M \left\{ a_{rn} f(x+\frac{2n-1}{2}\Delta) - a_{ln} f(x-\frac{2n-1}{2}\Delta) \right\}, \quad (3)$$

where  $\tilde{f}$  means the virtual value on nodes beyond the boundary. Next, the continuity condition for  $\partial E_z/\partial t = (\partial H_y/\partial x - \partial H_x/\partial y)/\varepsilon$  of the  $M$ th-order on the dielectric interface by using (2) is

$$\begin{aligned} \varepsilon_r^{(1)} b_{l0} \tilde{f}^{(1)}(x+\frac{\Delta}{2}) - \varepsilon_r^{(1)} b_{r0} \tilde{f}^{(1)}(x-\frac{\Delta}{2}) &= \varepsilon_r^{(1)} \left\{ \sum_{n=1}^M b_{rn} f(x+\frac{2n-1}{2}\Delta) - \frac{\partial H_x}{\partial y} \right\} \\ &\quad - \varepsilon_r^{(1)} \left\{ \sum_{n=1}^M b_{ln} f(x-\frac{2n-1}{2}\Delta) - \frac{\partial H_x}{\partial y} \right\}. \end{aligned} \quad (4)$$

For the continuity of  $\partial H_y/\partial t = (\partial E_z/\partial x)/\mu$  on the interface, it is

$$b_{l0} \tilde{f}^{(1)}(x+\frac{\Delta}{2}) - b_{r0} \tilde{f}^{(1)}(x-\frac{\Delta}{2}) = \sum_{n=1}^M \left\{ b_{rn} f(x+\frac{2n-1}{2}\Delta) - b_{ln} f(x-\frac{2n-1}{2}\Delta) \right\}. \quad (5)$$

(1a) is obtained from (3) and (4). The pair of (3) and (5) give (1b). Here, the coefficients for  $N=3$  and  $M=2$  in (1) are

$$\begin{aligned} a_{r0}(\delta) &= (15\Delta^3 - 46\delta\Delta^2 + 36\delta^2\Delta - 8\delta^3)/48\Delta^3, \\ a_{r1}(\delta) &= (15\Delta^3 + 14\delta\Delta^2 - 28\delta^2\Delta + 8\delta^3)/16\Delta^3, \\ a_{r2}(\delta) &= -(5\Delta^3 - 2\delta\Delta^2 - 20\delta^2\Delta + 8\delta^3)/16\Delta^3, \\ a_{r3}(\delta) &= (3\Delta^3 - 2\delta\Delta^2 - 12\delta^2\Delta + 8\delta^3)/48\Delta^3, \\ b_{r0}(\delta) &= -(\Delta - \delta)/\Delta^2, \quad b_{r1}(\delta) = (\Delta - 2\delta)/\Delta^2, \quad b_{r2}(\delta) = \delta/\Delta^2, \end{aligned} \quad (6)$$

where  $a_{ln}(\delta) = a_{rn}(-\delta)$  and  $b_{ln}(\delta) = -b_{rn}(-\delta)$ .